

# OVAL BRACELET WITH SURFACE DECORATIONS OF LINES AND INDENTATIONS MAH ANC. 2662 – LEADED BRONZE – LATE BRONZE AGE – SWITZERLAND

<b>Artefact name</b>	Oval bracelet with surface decorations of lines and indentations MAH anc. 2662
<b>Authors</b>	Marianne. Senn (Empa, Dübendorf, Zurich, Switzerland) & Christian. Degryny (HE-Arc CR, Neuchâtel, Neuchâtel, Switzerland)
<b>Url</b>	<a href="/artefacts/1224/">/artefacts/1224/</a>

## ∨ The object

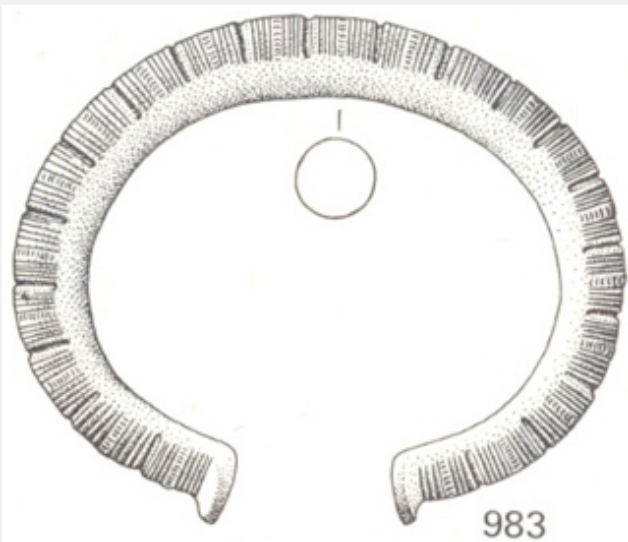


Fig. 1: Oval bracelet with surface decorations of lines and indentations (after Paszthory 1985, Tafel 82),

*Credit HE-Arc CR.*

## ∨ Description and visual observation

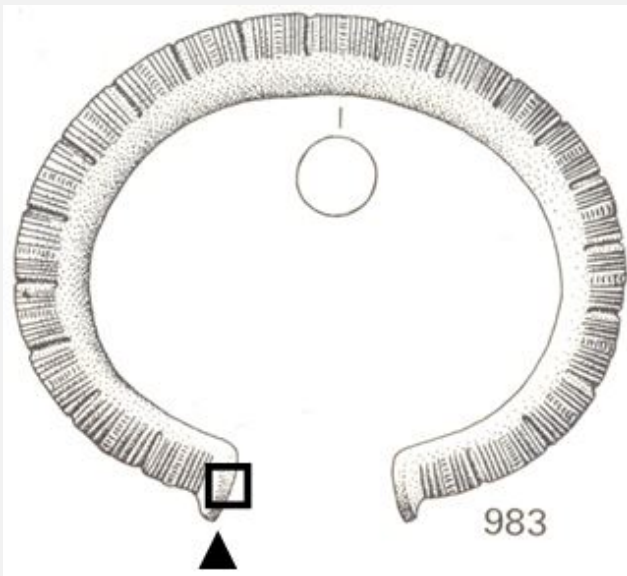
<b>Description of the artefact</b>	Bracelet decorated on the outside with surface decorations of lines and indentations (Paszthory 1985, 164 - Fig.1). It presents a dense, black patina. Dimensions: Ø = around 6.1cm; WT = 98g.
<b>Type of artefact</b>	Jewellery
<b>Origin</b>	Les Eaux-Vives, Genève, Geneva, Switzerland
<b>Recovering date</b>	Unknown
<b>Chronology category</b>	Late Bronze Age

chronology tpq	1000	B.C. ▾
chronology taq		---- ▾
Chronology comment	Hallstatt B2/3 (1000BC _ not defined)	
Burial conditions / environment	Lake	
Artefact location	Musées d'art et d'histoire, Genève, Geneva	
Owner	Musées d'art et d'histoire, Genève, Geneva	
Inv. number	MAH anc. 2662	
Recorded conservation data	N/A	

#### Complementary information

None.

#### Study area(s)



Credit HE-Arc CR.

Fig. 2: Location of sampling area,

#### Binocular observation and representation of the corrosion structure

None.

#### MiCorr stratigraphy(ies) – Bi

## Sample(s)

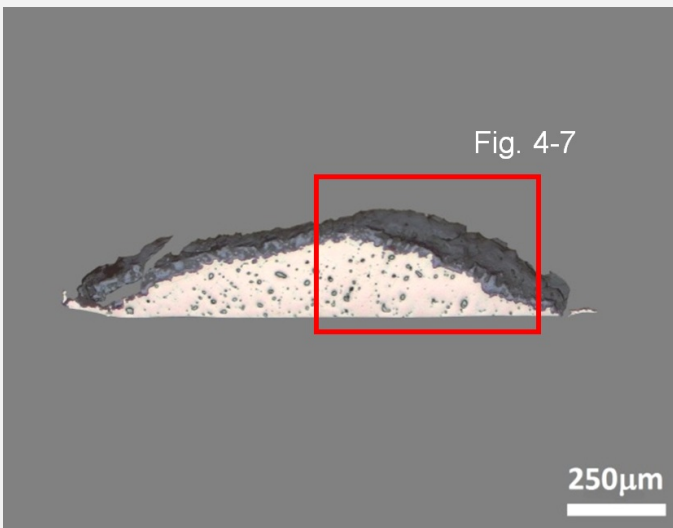


Fig. 3: Micrograph of the cross-section of the sample taken from the bracelet with surface decorations of lines and indentations showing the location of Figs. 4 to 7,

Credit HE-Arc CR.

<b>Description of sample</b>	Two samples were taken from this object – only one is presented here. The sample is a section from one end of the bracelet (Fig. 2). Its dimensions are: L = 1.3mm and W = 0.3mm. The corrosion layer is relatively thick (Fig. 3).
<b>Alloy</b>	Leaded Bronze
<b>Technology</b>	As-cast
<b>Lab number of sample</b>	MAH 77-110-1a
<b>Sample location</b>	Musées d'art et d'histoire, Genève, Geneva
<b>Responsible institution</b>	Musées d'art et d'histoire, Genève, Geneva
<b>Date and aim of sampling</b>	1977, study of black and iron rich surface deposit on the object

## Complementary information

None.

## Analyses and results

### *Analyses performed:*

Metallography (etched with ferric chloride reagent), Vickers hardness testing, ICP-OES, SEM/EDS.

## Non invasive analysis

None.

∨ Metal

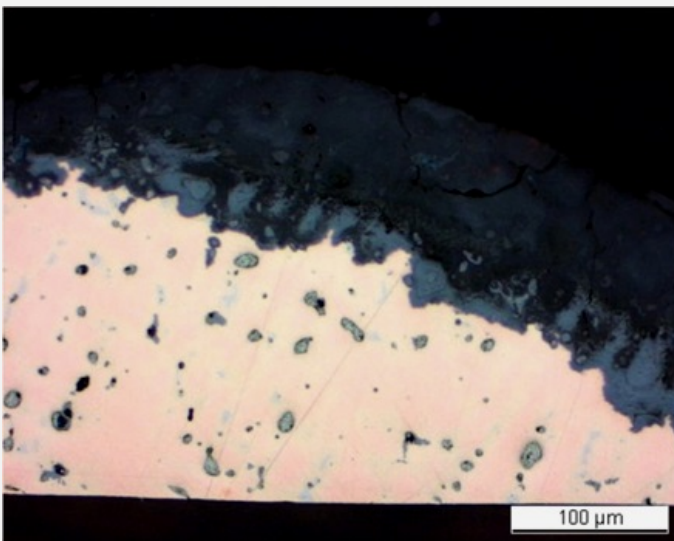
The remaining metal is a leaded bronze (Table 1) with low porosity, light and dark-grey inclusions (Fig. 4). In bright field the unetched alpha-delta eutectoid appears light-blue (Fig. 4). Etching reveals the dendritic structure of an as-cast metal (Fig. 5) with an average hardness of HV1 100. The inclusions appear as dark-grey (Pb-rich) and light-grey (copper sulphide) (Fig. 5 and Table 2) while the alpha-delta eutectoid is white (Fig. 5). The pink alpha phase is cored.

Elements	Cu	Sn	Pb	Sb	As	Ni	Ag	Zn	Fe	Co	Bi
mass%	87.62	6.98	4.36	0.42	0.23	0.18	0.13	0.04	0.03	0.02	0.02

Table 1: Chemical composition of the metal. Method of analysis: ICP-OES, Laboratory of Analytical Chemistry, Empa.

Elements	S	Cu	Pb	Total
Light-grey inclusion	21	82	<	103
Dark-grey inclusion	<	2	92	94

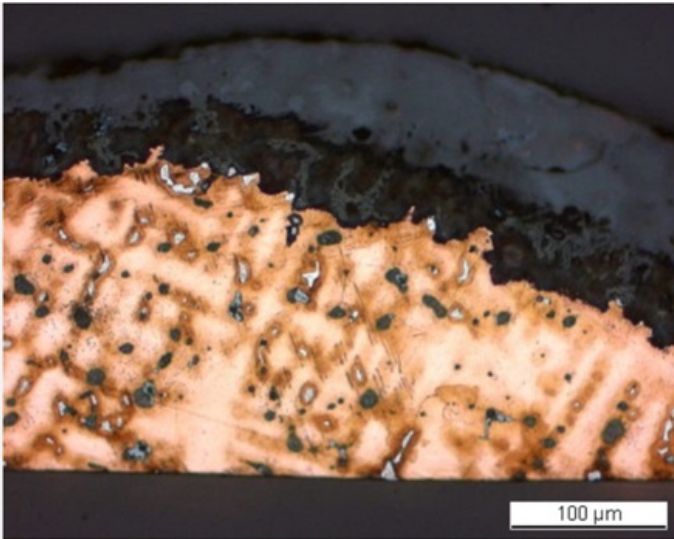
Table 2: Chemical composition (mass %, <: below the detection limit) of the inclusions on Fig. 4. Method of analysis: SEM/EDS, Laboratory of Analytical Chemistry, Empa.



Credit HE-Arc CR.

Fig. 4: Micrograph of the metal sample from Fig. 3 (detail), unetched, bright field. The metal is in pink, the Pb-rich inclusions in light-grey, the copper sulphide inclusions in dark-grey and the alpha-delta eutectoid in light-blue,

Fig. 5: Micrograph similar to Fig. 5, etched, bright field. The dendritic structure of the leaded bronze is revealed with the alpha-delta eutectoid in white and the alpha phase in pink. The colour difference of the alpha phase is due to coring,



Credit HE-Arc CR.

<b>Microstructure</b>	Dendritic structure with pores and inclusions
<b>First metal element</b>	Cu
<b>Other metal elements</b>	Ni, As, Ag, Sn, Sb, Pb

#### Complementary information

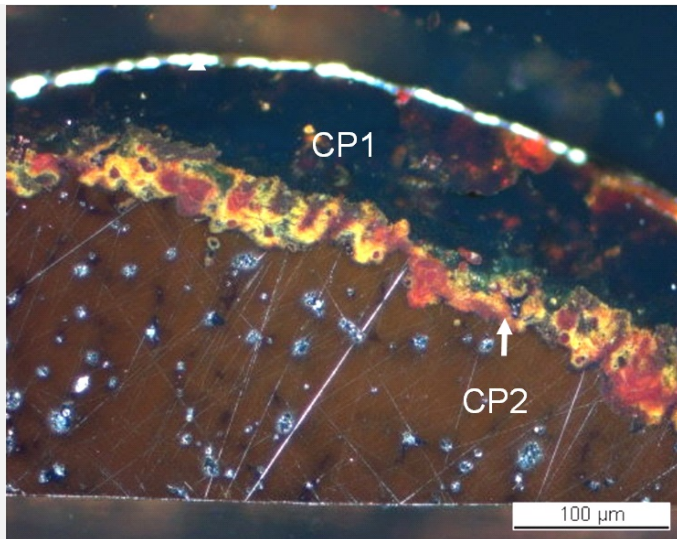
None.

#### Corrosion layers

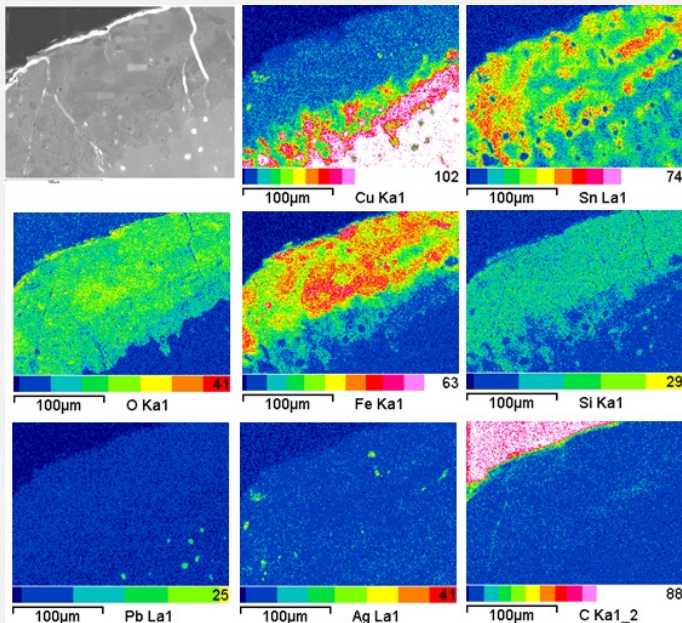
The corrosion crust has an average thickness of 80μm. It is composed of two layers (Fig. 6). The inner layer (CP2), which appears grey in bright field (Fig. 4), retains a Sn-rich dendritic ghost structure (Table 3 and Fig. 5). In polarized light, this layer is a mixture of reddish and yellow-brown corrosion products with some green areas (Fig. 6). The reddish parts have a composition similar to cuprite/Cu<sub>2</sub>O (Table 3). The adjacent dense, cracked layer, which appears dark-grey in bright field (CP1), is mainly composed of Fe<sub>2</sub>O<sub>3</sub> and Sn with Sn<sub>2</sub>O<sub>3</sub> and Fe-rich and Fe and O-rich zones contaminated with Si while being depleted of Cu (Fig. 8). In polarised light, it is dark, almost black with some red areas. In areas it contains Ag, Fe and Sn-rich inclusions with traces of Pb and Cu (Fig. 7 and Table 3).

Elements	O	Pb	Fe	Cu	Si	Sn	Ag	Total
CP1, light-grey in Fig. 7	40	6	8	21	4	<	<	79
CP1, dark-grey in Fig. 7	30	5	19	4	3	<	<	61
CP1, bright inclusion	5	10	45	2	<	28	28	118
CP2, dendritic ghost structure	39	6	17	32	3	<	<	97
CP2, reddish part	14	<	77	3	<	<	<	94

Table 3: Chemical composition (mass %, <: below the detection limit) of the corrosion layers from Figs. 6 and 7. Method of analysis: SEM/EDS, Laboratory of Analytical Chemistry, Empa.



Credit HE-Arc CR.



Credit HE-Arc CR.

Fig. 6: Micrograph similar to Fig. 4 and corresponding to the stratigraphy of Fig. 8, polarised light. From bottom left to top right: the metal in brown, the dendritic ghost structure in red, yellow-brown and green and the outer corrosion layer in black with some red areas. The thin white line is a crack,

Fig. 7: EDS elemental chemical distribution in an SEM image (detail of Fig. 4, reversed picture). Method of examination: SEM/EDS, Laboratory of Analytical Chemistry, Empa,

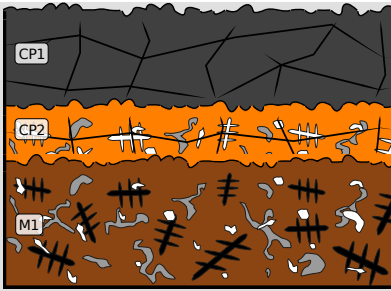
**Corrosion form** Uniform - selective  
**Corrosion type** Type II (Robbiola)

**Complementary information**

None.

∨ MiCorr stratigraphy(ies) – CS

Fig. 8: Stratigraphic representation of the sample taken from the bracelet with a dense, black lake patina in cross-section (dark field) using the MiCorr application. The characteristics of the strata are only accessible by clicking on the drawing that redirects you to the search tool by stratigraphy representation. This representation can be compared to Fig. 6, Credit HE-Arc CR.



#### ∨ Synthesis of the binocular / cross-section examination of the corrosion structure

None.

#### ∨ Conclusion

The surface of the cast leaded bronze has been replaced by a Fe/Sn-rich corrosion that retains a dendritic ghost structure. It is composed of a mixture of copper oxides (cuprite?) and a Sn-rich corrosion product (cassiterite?). The outer corrosion layer is composed of Fe-O and Sn-O-Fe areas depleted of Cu, but contaminated with Si. The enrichment in Fe seems to be the same as for the formation of patinas from lake contexts. However the outer corrosion layer was not formed in anaerobic conditions. Since the original surface is absent (destroyed) we refer to type corrosion 2 after Robbiola et al. 1998.

#### ∨ References

##### References on object and sample

1. Boll, P. (1991) Empa-Bericht n° 137'695/1991, not published.
2. Mottier, Y., Schweizer, F. (1977, 1991) Rapport du Laboratoire de recherche des musées d'art et d'histoire, not published.
3. Paszthory, K. (1985) Der bronzezeitliche Arm- und Beinschmuck in der Schweiz. Prähistorische Bronzefunde X-Bd. 3, München 1985, 164, Tafel 82.

##### References on analytic methods and interpretation

4. Mottier, Y., Schweizer, F. (1977, 1991) Rapport du Laboratoire de recherche des musées d'art et d'histoire, not published.
5. Robbiola, L., Blengino, J-M., Fiaud, C. (1998) Morphology and mechanisms of formation of natural patinas on archaeological Cu-Sn alloys, Corrosion Science, 40, 12, 2083-2111.